ORAL REFERENCE ICF0744

FOREIGN OBJECT DAMAGE AND HIGH-CYCLE FATIGUE THRESHOLDS IN TI-6AL-4V

J. O. Peters[**], B. L. Boyce, J. M. McNaney and R. O. Ritchie

Department of Materials Science and Engineering,
University of California, Berkeley, CA 94720-1760

ABSTRACT

The objective of this study is to define limiting threshold conditions for high cycle fatigue (HCF) in the presence of foreign object damage (FOD) in an engine Ti-6Al-4V alloy. Impacts in the form of FOD were simulated by firing steel spheres onto tensile fatigue specimens at velocities of 200 to 300 m/s. Such FOD was found to reduce the fatigue strength of the alloy, primarily due (i) stress concentration, (ii) microcrack formation, (iii) impact-induced plasticity and (iv) tensile residual stresses associated with the impact damage. Two groups of fatigue failures could be identified. The first group initiated directly at the impact site, and can be readily described through a Kitagawa-Takahashi approach, where the limiting threshold conditions are defined by the stress-concentration corrected smooth-bar fatigue limit (at microstructurally-small crack sizes) and a "worst-case" fatigue crack growth threshold (at larger "continuum-sized" crack sizes). The second group of failures was caused by fatigue cracks that initiated at locations remote from the impact site in regions of high tensile residual stresses. By evaluating the effect of such residual stresses as a superimposed mean stress, specifically by conducting smooth-bar *S-N* tests at load ratios between -1 and 0.8, it was found that simple superposition of the applied and initial residual stresses provided a significant contribution to the FOD-induced reduction in fatigue strength by affecting the *local* load ratio. Such factors are considered in a modified Kitagawa-Takahashi approach to provide a basis for the effect of FOD on HCF failures in Ti-6Al-4V. To evaluate the role of surface treatments to enhance high-cycle fatigue resistance, fatigue specimens were also laser shock peened prior to FOD-impact and subsequent fatigue loading. The initial results of these HCF failures of laser shock peened samples are briefly discussed.

KEYWORDS

Ti-6Al-4V, foreign object damage, high cycle fatigue, residual stress, fatigue crack initiation, fatigue crack growth threshold

INTRODUCTION

High-cycle fatigue (HCF) of turbine engine disk and blade components represents one of the major concerns limiting with the readiness and safety of military aircraft. Since *in-flight* HCF conditions invariably involve high cyclic frequencies, small crack sizes and (depending on blade location) very high mean stress levels, a preferred approach for design against HCF can be considered in terms of the concept of a threshold for no fatigue crack growth [1-3]. Foreign object damage (FOD) by small hard particles has been identified as a key factor associated with such HCF related failures in titanium alloy blades [1,2]. Specifically, FOD has been found to reduce the fatigue strength of fan and compressor blades, principally by causing stress-raising notches and microcracks [2] at impact sites; this, in association with the plastic deformation and tensile residual stresses resulting from such impacts [1], can lead to the early nucleation and growth of fatigue cracks.

[**] Now with the Department of Physical Metallurgy and Materials Technology, Technical University Hamburg-Hamburg, 21071 Hamburg, Germany

Recent studies [4,5] on the HCF properties of a Ti-6Al-4V blade alloy, where FOD was simulated using high-velocity impacts of steel shot on a flat surface, have focused on the definition of threshold conditions for crack initiation and growth on subsequent fatigue cycling. The mechanistic effect of FOD was considered in terms of (i) the possibility of forming microcracks in the damage zone, (ii) the stress concentration associated with the FOD-induced notches, (iii) microstructural damage from FOD-induced plastic deformation, and (iv) the localized presence of tensile residual hoop stresses in the vicinity of the impact site. Although all these factors play an important role, a pivotal effect of FOD in reducing fatigue life in Ti-6Al-4V appears to be the formation, at high impact velocities, of damage-induced microcracks; on subsequent cycling, these act as preferred sites for the initiation of fatigue cracks in the pile-up of material around the rim of the impact crater, depending upon the relative magnitude of the residual stresses in the vicinity of the impact. For high applied stress ranges, HCF failures initiate directly *at* the impact site, whereas at correspondingly low applied stresses ranges, they initiate in locations *away* from the impact site.

In analyzing the high stress failures, it was found that FOD-initiated microcracks, together with the stress concentration of the indent, were the prime reasons that the HCF failures initiated at the FOD sites. The microcracks (some as small as 1 μm) grew at applied stress intensities as low as ΔK = 1 MPa√m, which is well below the "worst-case" ΔK_{TH} threshold in bi-modal Ti-6Al-4V [6] of 1.9 MPa√m for "continuum-sized" cracks, i.e., for cracks larger than the characteristic microstructural size-scales. Thus, although the "worst-case" threshold, which is determined at $R \rightarrow 1$ to minimize crack closure, provides a critical lower-bound for the growth of HCF cracks in bi-modal Ti-6Al-4V, it only applies for "continuum-sized" cracks, which in this microstructure are larger than ~50-100 μm in length. Since the microcracks associated with impact damage are more than an order of magnitude smaller than this, an alternative approach is proposed to describe the threshold HCF conditions in the presence of FOD based on a Kitagawa-Takahashi diagram, where the limiting conditions for HCF are defined in terms of the stress concentration-corrected smooth-bar fatigue limit (at microstructurally-small cracks sizes) and the "worst-case" threshold (at larger, "continuum-sized" crack sizes).

In contrast to HCF failures under high applied stresses, at low applied stress ranges failures were caused by fatigue cracks that initiated at locations remote from the impact site, specifically in regions of high tensile residual stresses. It is the purpose of this paper to examine the role of the relative magnitudes of the applied and residual stresses in dictating the sites for the initiation of HCF failures in impact-damaged Ti-6Al-4V, and to provide a methodology to describe the limiting threshold conditions for such failures at both low and high applied cyclic stresses. To achieve this objective, the residual stresses in the vicinity of the damage sites are computed numerically [7] and measured experimentally using synchrotron x-ray micro-diffraction. Such stresses are considered to affect the local load ratio for subsequent fatigue cracking, which is evaluated by determining smooth-bar stress-life (*S-N*) curves for load ratios from R = -1 to 0.8. Using such results, a modified Kitagawa-Takahashi approach is presented to provide a rational basis for the effect of FOD on HCF failures in Ti-6Al-4V at both high and low applied stresses.

Additionally, we briefly consider the effect of laser shock peening (LSP) as a surface treatment to improve resistance to FOD-induced failures under HCF cycling [1,8]. In this study, the flat surfaces of fatigue samples were prepared by LSP processing prior to FOD event, and the subsequent fatigue lives compared to of samples without such surface treatment.

EXPERIMENTAL PROCEDURES

The Ti-6Al-4V alloy investigated, of composition (in wt.%) Ti-6.3Al-4.19V-0.19Fe-0.19O-0.013N-0.0041H, was from the forgings produced specifically for the U.S. Air Force National HCF Program. The bi-modal (solution treated and overaged) microstructure of this material, consists of ~60 vol.% primary α (grain size ~20 μm) within a lamellar α+β matrix. The alloy has yield and tensile strengths of 915 and 965 MPa, respectively, with a reduction in area of 45%, based on tests parallel to the length of the plate [4].

Foreign object damage was simulated by firing 1.0 mm or 3.2 mm diameter chrome-hardened steel spheres onto a flat specimen surface of tensile fatigue (so-called modified K_B, details are given in Ref. [4]) specimens at an angle of 90º at velocities of 200 and 300 m/s using a compressed-gas gun facility. Impact velocities of 200 to 300 m/s represent typical in-service impact velocities on aircraft engine fan blades. The impact damage craters are also typical of those seen in service, with root radii similar to those of actual damage sites [2].

To evaluate the effect of surface treatments on the HCF resistance, the gauge and transition section of modified K_B specimens were laser shock peened to induce compressive residual stresses to approximately 500 μm deep on each side.

Following impacting with the steel spheres to simulate FOD, the damaged regions were examined in a high-resolution, field-emission scanning electron microscope (SEM), prior to cycling at maximum stress values between 225 and 500 MPa at R = 0.1 and 0.5 (with a sinusoidal waveform).

Stress-intensity threshold conditions for no crack growth of small cracks at the impact site were defined based on the relationship of Lukáš [9] for small cracks at notches; for further details see Ref. [5]. Because the FOD-initiated microcracks have lengths ($2c$ ~ 1 to 50 μm) that are comparable to the scale of local plasticity, there may be a degree of uncertainty in the calculation of their driving forces. However, maximum plastic zone sizes are only ~ 0.2 to 1 μm for 1 to 10 μm sized cracks at ΔK ~ 1 - 2 MPa√m, such that conditions are close to that of small-scale yielding. The contribution of the residual stresses is not included in this ΔK calculation since these stresses do not change the stress intensity *range*. They do, however, affect the mean stress and hence alter the local load ratio, as is examined below. Indeed, initial estimates of the magnitude and gradient of the residual stresses have been computed [7] and are experimentally measured in this study.

RESULTS AND DISCUSSION

Simulation of foreign object damage

Damage sites on the flat surface of the rectangular gauge section of K_B specimens, resulting from 300 m/s impacts with 1 and 3.2 mm steel shot, are shown in Figs. 1a,b. Increasingly severe damage states have been previously reported with increasing impact velocity for the bi-modal Ti-6Al-4V [4,5]. For impact velocities in excess of ~250 m/s, pile-up of material (Fig. 1) at the crater rim resulted in multiple formation of microcracking (insert in Fig. 2). Moreover, circumferentially-oriented intense shear bands were formed, emanating from the surface of the impact crater. The microcracks (~2 to 50 μm) were found to provide the nucleation sites for crack growth on subsequent cycling (Fig. 2), although such microcracking was not seen at slower 200 m/s impacts. For this reason, we believe that low velocity or quasi-static indentations do not provide a realistic simulation of FOD.

In addition to the formation of the FOD-induced microcraks, the presence of tensile residual stresses at locations remote from the impact site was also of importance for crack initiation, especially for failures in the 10^7 to 10^8 cycles regime. These tensile stresses, measured using synchrotron x-ray micro-diffraction techniques at the side faces of the K_B specimens, counterbalance the compressive residual stress field directly beneath the indentation, as predicted numerically [7]. The estimated distributions of these FOD-induced stresses in K_B specimens are shown in Figs. 3a and b for 300 m/s impacts using 1 mm and 3.2 mm steel shot, respectively, and display tensile residual stresses (in longitudinal direction) as high as ~220 MPa (σ_{33}/σ_y = 0.24) to 385 MPa (σ_{33}/σ_y = 0.42), where σ_y is the yield stress, and σ_{33} the normal residual stress in longitudinal direction. The effect of such residual stresses on fatigue crack initiation and the fatigue crack growth thresholds is discussed below.

Fatigue properties

Stress-life (S-N) data in Fig. 4 clearly show the detrimental effect of FOD on the fatigue strength of bi-modal Ti-6Al-4V. The reduced lifetimes following impact damage was seen for both projectile sizes and at both low and high load ratios (R = 0.1 and 0.5). As discussed previously [8-10], this detrimental effect of FOD can be considered in terms of premature fatigue crack initiation resulting from (i) the stress concentration of the indent, (ii) FOD-induced microcracking, (iii) plastically-deformed microstructure and (iv) tensile residual stresses that result from the impact.

Two groups of failures can be identified in Fig. 4, dependent upon the magnitude of the applied stresses relative to the tensile residual stresses. At high applied stresses, HCF failures initiate directly *at* the impact crater. For 300 m/s impact velocities where FOD-induced microcracks were formed, fatigue cracking initiated from these microcracks at the crater rim (surface crack lengths are indicated at groups of data points); at 200 m/s impact velocities, fatigue cracking initiated at the base of indent site where the stress concentration is higher (compared to that at the crater rim) [5]. In contrast, at low applied stresses (and lower impact velocities), where FOD-induced microcracks were not formed or were much smaller, fatigue cracks were found to initiate *away* from the indent crater, in regions of relatively high tensile residual stresses.

An example of fatigue crack initiation at low applied cyclic stresses (σ_{max} = 325 MPa, R = 0.1) in regions remote from the damage site in the interior of a K_B specimen is shown in Figs. 5a and b for 300 m/s impacts of, respectively, 1 and 3.2 mm diameter shot. A further example (at σ_{max} = 300 MPa, R = 0.1), where initiation occurred close to surface at the side face of the specimen is shown in Fig. 5c. In all cases, fatigue cracking initiated in regions of the high tensile residual stresses away from the indent; specifically, these stresses were ~300 MPa, based on synchrotron x-ray diffraction measurements [10] and numerical computations (Fig. 3).

The tensile residual stresses also elevate the load ratio, when simply superimposed on the applied far-field fatigue loading. Based on FOD-related failures at applied cyclic stresses of 270 to 300 MPa (R = 0.1) and 250 MPa (R = 0.5), superimposing a measured tensile residual stress of ~300 MPa increases these R-ratios from 0.1 to ~0.5 and from 0.5 to ~0.7, assuming no relaxation. The corresponding increase in the maximum stress by this superposition is marked by arrows in the S-N diagram shown in Fig. 4. From these S-N results it is

clear that simple superposition of initial tensile residual stress onto applied far-field stress provides a significant contribution to the reduction in fatigue life due to FOD through its effect in elevating the local *R*-ratio.

Threshold conditions based on the Kitagawa diagram

For high applied stress ranges (relative to the magnitude of tensile residual stresses) and in the presence of relatively large impact-induced microcracks (~ 30 to 50 μm), it was found that fatigue failures at 10^5 to 10^6 cycles initiated directly at the impact site. These fatigue failures (shown as closed symbols in Fig. 6) have been described in our previous work [5] through the use of fatigue crack growth threshold concept and the Kitagawa-Takahashi diagram [11]. Here, the limiting threshold conditions were defined by the stress-concentration corrected smooth-bar fatigue limit (at microstructurally-small crack sizes) and a "worst-case" fatigue crack growth threshold (at larger "continuum-sized" crack sizes). A more favorable representation of the failure envelopes for the two load ratios of 0.1 and 0.5 in Fig. 10 can be made using the El Haddad *et al*. [12] empirical quantification of Kitagawa approach, which introduces a constant, termed the intrinsic crack length, $2c_o$, such that the stress intensity is defined as $\Delta K = Y \Delta\sigma \, [\pi(2c + 2c_o)]^{1/2}$, where Y is the geometry factor.

To account for residual stresses in this approach to describe the limiting threshold conditions for FOD-initiated HCF failures in Ti-6Al-4V, the effective *R*-ratio in the diagram has to be corrected for the presence of such residual stresses. Using the fatigue failures plotted in Fig. 10 as data points at surface crack lengths of $2c$ = 1 μm, and superimposing the measured tensile residual stress of ~300 MPa, the *R*-ratios are increased from 0.1 to ~0.5 and from 0.5 to ~0.7 at far-field stress range of ~300 MPa. Accordingly, such failures at both load ratios can still be described by the proposed Kitagawa-Takahashi approach, provided the limited conditions are given by the stress concentration *and* residual stress corrected smooth-bar fatigue limit at small crack sizes and the "worst-case threshold" for larger crack sizes.

The full quantitative effect of the FOD-induced residual stresses on fatigue failures at 10^5 to 10^6 cycles, however, is still under study. Although simple superposition of the residual and applied stresses was considered above, our recent *in situ* x-ray micro-diffraction results have indicated that during the first few fatigue cycles, significant relaxation of the residual stresses occurs *at* the base and rim of the impact crater, but *not at* locations a crater diameter or so away where fatigue cracks initiate under low applied stresses. This effect is currently under investigation using both *in situ* x-ray studies and numerical computation.

Laser Shock Peening

Laser shock peening (LSP) has been proposed as an effective means to improve the fatigue strength of titanium turbine blades, especially to enhance the HCF resistance to FOD [1,8]. A prime cause for this effect is that LSP can induce significant compressive residual stresses below the surface, which inhibits the propagation of FOD-related surface fatigue cracks. The positive effect of LSP prior to 200 m/s (3.2 mm shot) impacts is shown in Fig. 7, where it can be seen that the LSP process resulted in fatigue life extension of more than one order of magnitude. However, at higher impact velocities of 300 m/s (3.2 mm shot), LSP had little influence on HCF resistance (Fig. 7). As the impact crater sizes were essentially identical for non-LSP and LSP treated fatigue samples at this velocity, the similar fatigue lives appear to be the result of the deep impact penetration compared to the depth of LSP-induced compressive residual stresses. Currently, both experimental and numerical studies are focused on quantifying residual stress gradients after the LSP process and following FOD in order to explain limited benefits of LSP for the high velocity impacts.

SUMMARY AND CONCLUSIONS

Based on a study of the role of foreign object damage in affecting the high-cycle fatigue of an engine Ti-6Al-4V alloy with bi-modal microstructure, the prominent conclusions are:

1. Foreign object damage, simulated by high-velocity (200-300 m/s) impacts of steel spheres (1 and 3.2 mm shot) on a flat specimen surface, markedly reduced the HCF resistance, primarily by inducing sites for the premature initiation of fatigue cracks on subsequent cycling.
2. Premature crack initiation was caused by a number of factors: (i) the stress concentration due to the FOD indentation, (ii) the creation (at highest impact velocities only) of microcracks at the impact crater rim, (iii) microstructural damage from FOD-induced plastic deformation, and (iv) the localized presence of tensile residual stresses around the indent.
3. Two groups of FOD-induced HCF failures could be identified. The first group involved fatigue crack initiation directly at the impact site and caused failures within 10^5 to 10^6 cycles. The proposed criteria for such failures has been described by a modified Kitagawa-Takahashi approach, where the limiting threshold conditions are defined by the stress-concentration corrected smooth-bar fatigue limit (at

microstructurally-small crack sizes) and a "worst-case" fatigue crack growth threshold (at larger "continuum-sized" crack sizes).

4. The second group of failures at 10^7 to 10^8 cycles initiated at locations remote from impact damage in regions of high tensile residual stresses. Accordingly, the modified Kitagawa-Takahashi approach proposed above must be corrected for the presence of tensile residual stresses, in a first approximation by simple superposition of applied and residual stresses, to account for such failures. With this correction, this approach provides a rational basis for the effect of foreign object damage on high cycle fatigue failures in Ti-6Al-4V.
5. Laser shock peening (LSP) prior to FOD event was found to improve the HCF resistance following FOD, but only for lower impact velocities (200 m/s); no beneficial effect of LSP was found for high velocity impacts (300 m/s).

ACKNOWLEDGEMENTS

This work was supported by the Air Force Office of Science and Research, Grant No. F49620-96-1-0478, under the Multidisciplinary University Research Initiative on "High Cycle Fatigue" to the University of California, Berkeley. Special thanks are due to Prof. J. W. Hutchinson and Mr. X. Chen for providing us with their results prior to publication, and to Dr. D. M. Corbly and Mr. S. R. Mannava (GEAE) for helpful discussions and for the laser shock peening of our fatigue samples.

REFERENCES

1. Nicholas, T. (1999) *Int. J. Fatigue* 21, S221.
2. Hudak, S.J., Chan, K.S., McClung, R.C., Chell, G.G., Lee, Y.-D., Davidson, D.L. (1999) *High Cycle Fatigue of Turbine Blade Materials*, Final Technical Report UDRI Subcontract No. RI 40098X SwRI Project No. 18-8653.
3. Ritchie, R.O. (1996). In: *Proc. ASME Aerospace Division.* Chang, J.C.I., Coulter, J., Brei, D., Martinez, W.H.G., Friedmann, P.P. (Eds). AD-Vol. 52, ASME, Warrendale, PA, pp. 321-333.
4. Peters, J.O., Roder, O., Boyce, B.L., Thompson, A.W., Ritchie, R.O. (2000) *Metall. Mater. Trans. A.* 31A, 1571.
5. Peters, J.O., Ritchie, R.O. (2000) *Eng. Fract. Mech.* 67, 193.
6. Ritchie, R.O., Davidson, D.L., Boyce, B.L., Campbell, J.P., Roder, O. (1999) *Fat. Fract. Eng. Mat. Struct.* 22, 621.
7. Chen, X., Hutchinson, J.W. (2001) Unpublished research. Harvard University.
8. Ruschau, J.J., John, R., Thompson, S.R., Nicholas, T. (1999) *Int. J. Fatigue* 21, S199.
9. Lukáš, P. (1987) *Eng. Fract. Mech.*26, 471.
10. Boyce, B.L., Chen, X., Hutchinson, J.W., Ritchie, R.O. (2001) *Mechanics of Materials*, 33, 441.
11. Kitagawa, H., Takahashi, S. (1976) In: *Proc. Second Intl. Conf. on Mechanical Behavior of Materials,* ASM, Metals Park, OH, pp. 627-31.
12. El Haddad, M.H., Topper, T.H., Smith, K.N. (1979) *Eng. Fract. Mech.* 11, 573.

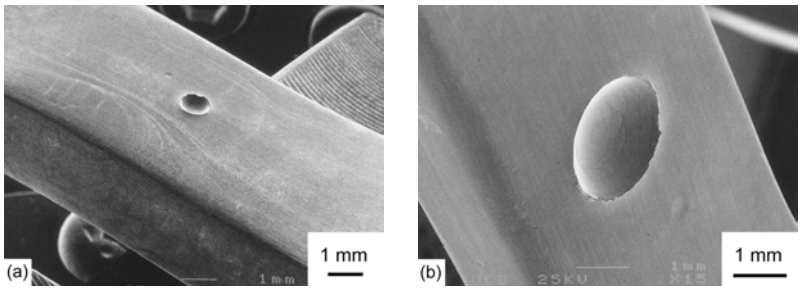

Fig. 1 Gauge section of modified K_B specimens for simulated FOD studies after high-velocity 300 m/s impact using (a) 1.0 mm diameter steel sphere and (b) 3.2 mm diameter steel sphere (normal impact angle).

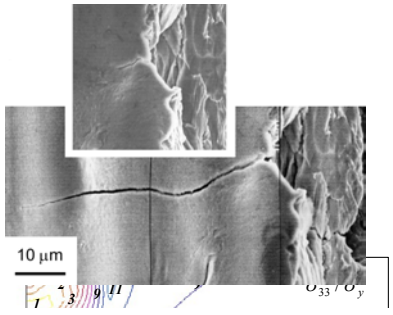

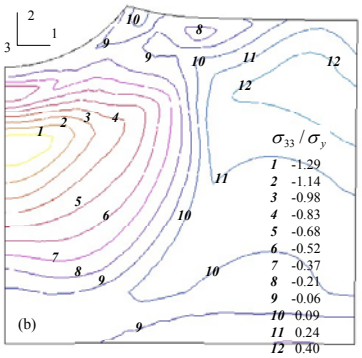

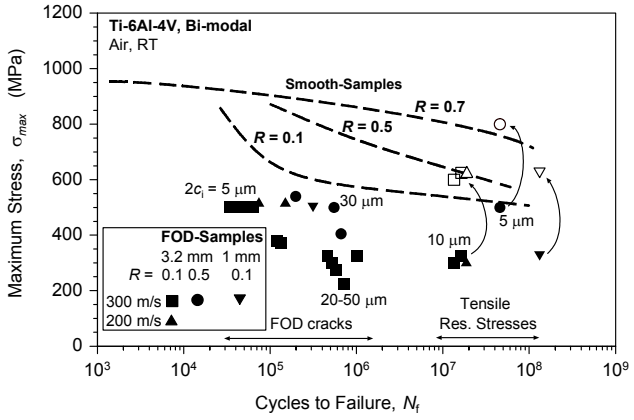

Fig. 4 *S-N* data show reduced fatigue life due to simulated FOD as compared to smooth-bar specimens. $2c_i$ is the surface crack length of FOD-induced microcracks. For failures at 10^7 - 10^8 cycles, the effect of local tensile residual stress (~300 MPa) in increasing the local maximum stress (and hence the local load ratio) has been illustrated by arrows and open symbols.

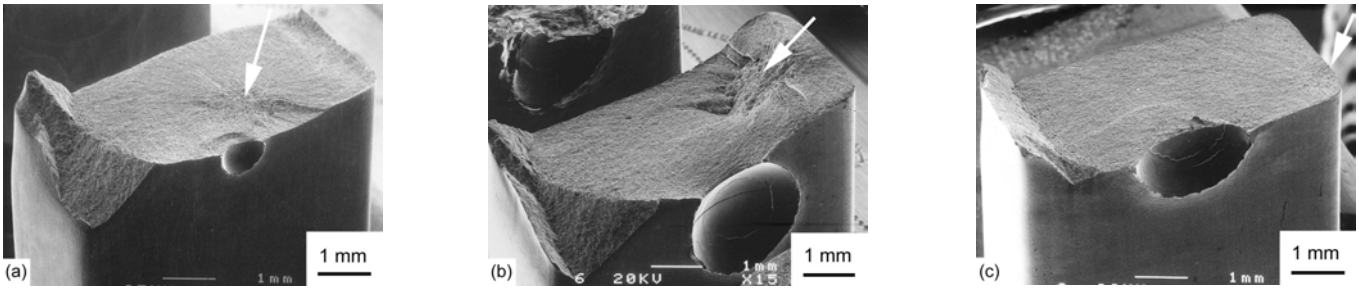

Fig. 5 Lower stress fatigue loading after 300 m/s impact using 1 mm or 3.2 mm diameter steel shot caused crack initiation away from the indent site (marked by arrows): (a) 1 mm steel shot, nominally applied σ_{max} = 325 MPa, R = 0.1, N_F = 1.3 x 10^8 cycles, (b) 3.2 mm steel shot, nominally applied σ_{max} = 325 MPa, R = 0.1, N_F = 1.6 x 10^7 cycles, and (c) nominally applied σ_{max} = 300 MPa, R = 0.1, N_F = 1.3 x 10^7 cycles.

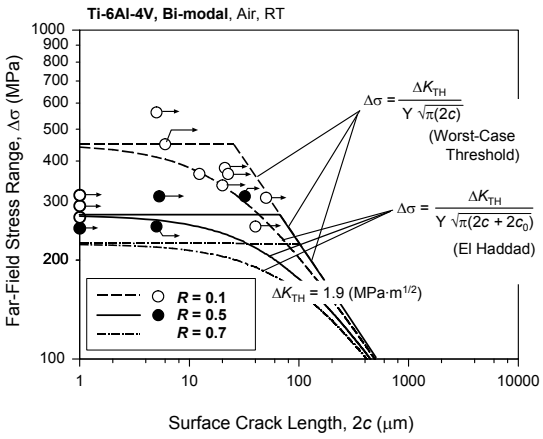

Fig. 6 Modified Kitagawa-Takahashi diagram representing the threshold crack-growth conditions (da/dN = 10^{-11}-10^{-10} m/cycle) at R = 0.1 and 0.5 for FOD-induced small-cracks in bimodal Ti-6Al-4V. Plotted is the threshold stress range as a function of surface crack length. Data points are corrected for the stress concentration of the FOD indents.

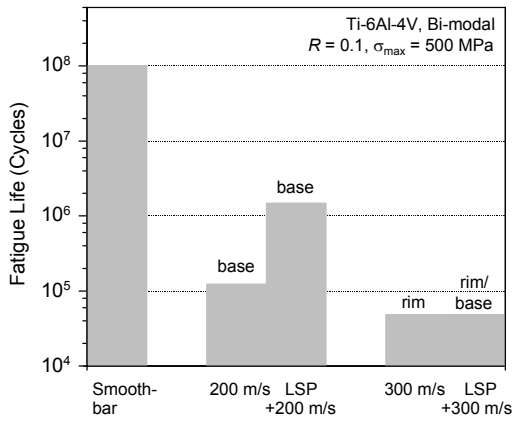

Fig. 7 Histogram showing the effect of laser shock peening (LSP) prior to the FOD event. FOD was simulated using 3.2 mm steel shot at velocities of 200 and 300 m/s. The sites of crack initiation, at base or rim at impact crater, are indicated.